

Interpretable Non-Destructive Discrimination of Japanese Bast Fibers via Micro-Hyperspectral Imaging

Yexin Zhou^{1,*}, Yoichi Ohyanagi², Akiko Iwata², Koji Shibazaki²

¹ Life and Culture Department, Seirei Women's Junior College, Akita, Japan

² Faculty of Fine Arts, Aichi University of the Arts, Nagakute, Japan

INTRODUCTION & AIM

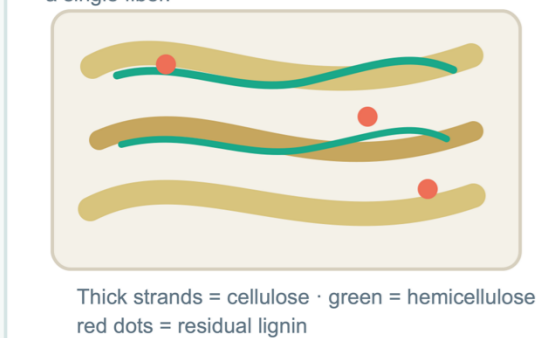
- Background:** Conservation repairs need fiber-compatible materials — a species mismatch causes secondary damage at the repair interface. Yet the standard JIS P8120 iodine-staining test is destructive and unsuitable for heritage objects.
- Gap:** Macroscopic HSI / AI screening reads only surface morphology and offers little physicochemical interpretability; intrinsic single-fiber spectral signatures remain uncharacterized.
- Aim:** Assess the feasibility of micro-hyperspectral imaging (Micro-HSI) with chemometrics for non-destructive, interpretable, species-level discrimination of three Japanese bast fibers — Kozo, Mitsumata, and Gampi.

Fiber Components & the Spectral Clues for Discrimination

Cellulose is nearly identical across species — discrimination comes from what residue remains and how it bonds

Bast fiber = three components

Within paper, the components intertwine into a single fiber.



Thick strands = cellulose - green = hemicellulose
red dots = residual lignin

Cellulose
The plant "skeleton" — paper strength and brightness.

Hemicellulose
The "binder" between cellulose chains — flexibility.

Lignin
The plant "glue" — residues cause yellowing & decay.

In one line
The cellulose skeleton is shared, so discrimination reads small differences in residual lignin and polysaccharide bonding from light near 400–450 nm and 835 nm.

The key to discrimination

Cellulose is highly similar across the three species, so the discriminating signal lies here:

Residual lignin
small residual glue

Polysaccharide network

Why washi-making reduces lignin

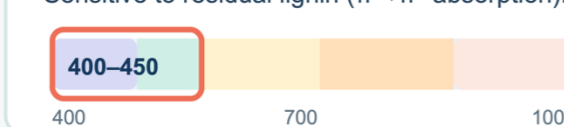
Steam / cook → Remove de-lignify

But removal is never identical across species — these residual differences surface in the spectrum.

Two spectral regions carry most of the discriminating information

Around 400–450 nm

The violet-to-blue edge of the visible range. Sensitive to residual lignin (π→π* absorption).



Around 835 nm

In the near-infrared range. Captures O–H / C–H overtones of the polysaccharides.

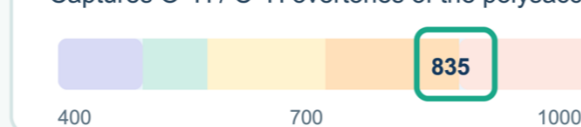


Fig. 1. Physicochemical basis and spectral interpretability for the discrimination of Japanese bast fibers. Fiber identification is based on two key diagnostic spectral regions: residual lignin absorption (≈400–450 nm) and polysaccharide overtone bands (≈835 nm). Although Kozo, Mitsumata, and Gampi share a common cellulose skeleton, subtle variations in residual lignin content and polysaccharide network structure, arising from species-specific chemical composition and processing, provide the spectral basis for their discrimination.

METHOD

- Samples:** 3 bast fibers × 6 pure, additive-free specimens from an authenticated 1973 reference archive; 10 ROIs per specimen = 60 ROI spectra per class (18 specimens total).
- Acquisition:** Push-broom HSI camera (NH-9) on an upright microscope, 50× objective, 350–1100 nm, 5 nm resolution.
- Pre-processing:** Dynamic normalization → Savitzky–Golay 1st derivative → CV-based window (400–1000 nm) → Z-score.
- Chemometrics:** PCA (unsupervised structure) and LDA (supervised discrimination), validated by Leave-One-Specimen-Out CV — one whole specimen held out per fold to avoid ROI data leakage.

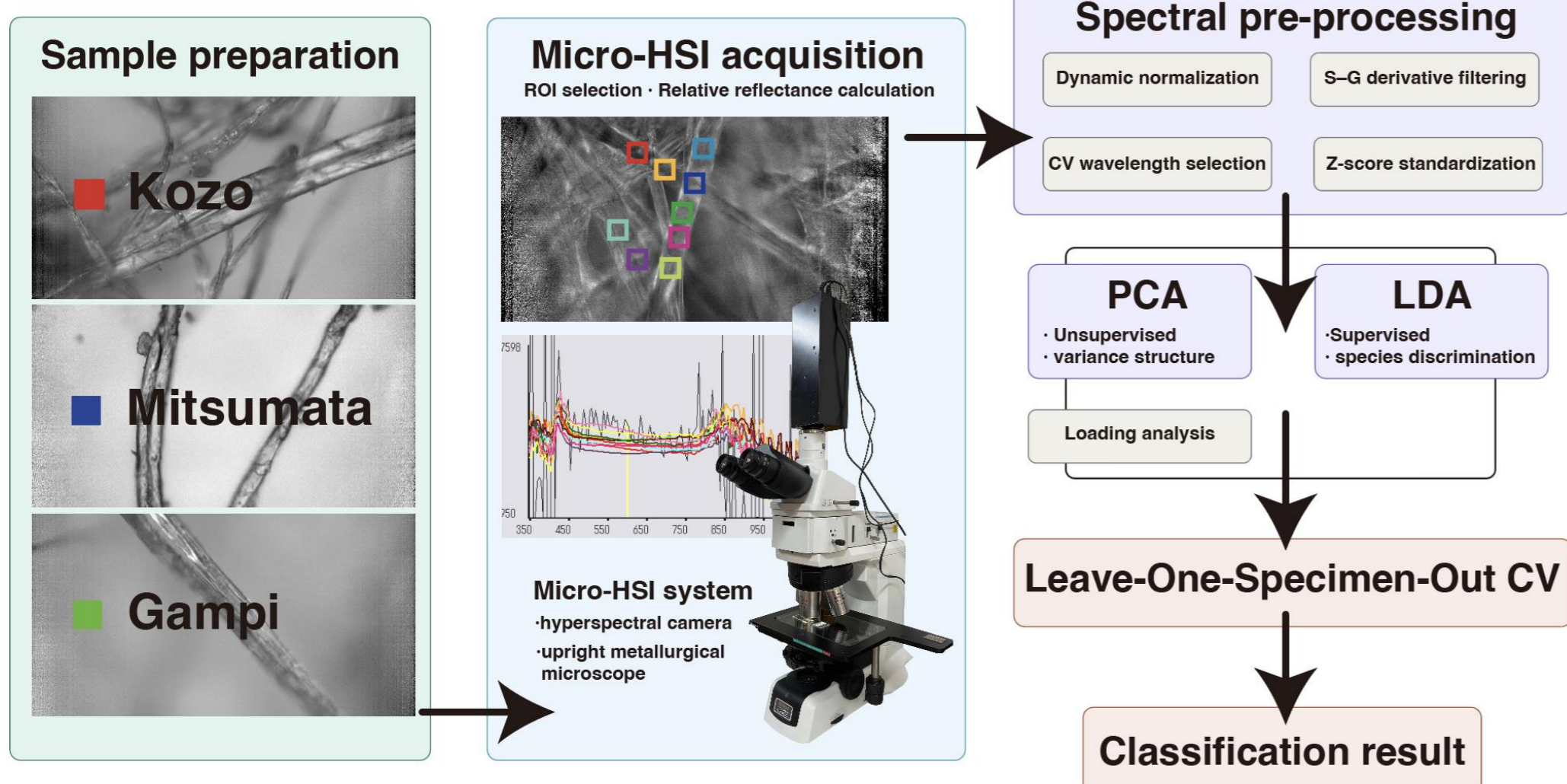


Fig. 2. Schematic overview of the analytical workflow. Three Japanese bast fibers—Kozo (red), Mitsumata (blue), and Gampi (green)—were analyzed using a Micro-HSI system consisting of a hyperspectral camera and an upright metallurgical microscope. Reflectance spectra were extracted from selected ROIs, followed by spectral pre-processing (dynamic normalization, Savitzky–Golay first derivative, CV-based wavelength selection, and Z-score standardization). Chemometric analyses were then performed using PCA and LDA, and classification performance was evaluated by Leave-One-Specimen-Out Cross-Validation (LOSO-CV).

RESULTS & DISCUSSION

- PCA:** 95% confidence ellipses overlap heavily (PC1–3 = 62.5% variance) — the shared cellulose matrix masks species differences.
- LDA:** Resolves all three fibers into distinct clusters (LD1 73.2%, LD2 26.8%).
- Diagnostic bands:** Lignin π→π* transition (400–450 nm) and NIR O–H / C–H polysaccharide overtones (≈835 nm).
- Accuracy:** LOSO-CV = 77.8%; Kozo classified error-free (F1 = 1.00); Mitsumata and Gampi F1 = 0.67 each.
- Confusion:** All errors fall within the chemically similar, low-lignin Mitsumata–Gampi pair.

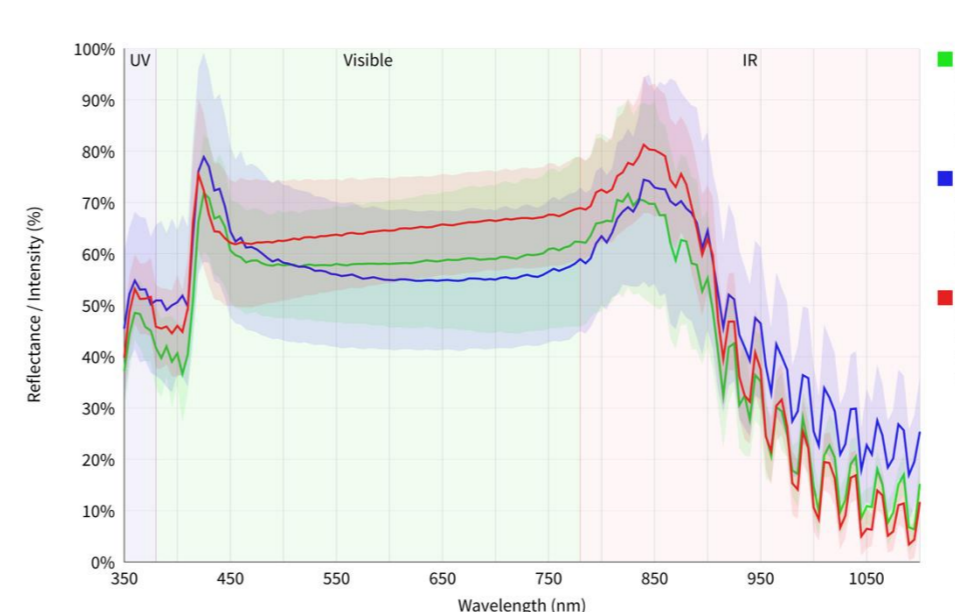


Fig. 3. Dynamically normalized reflectance spectra of the three bast fibers.

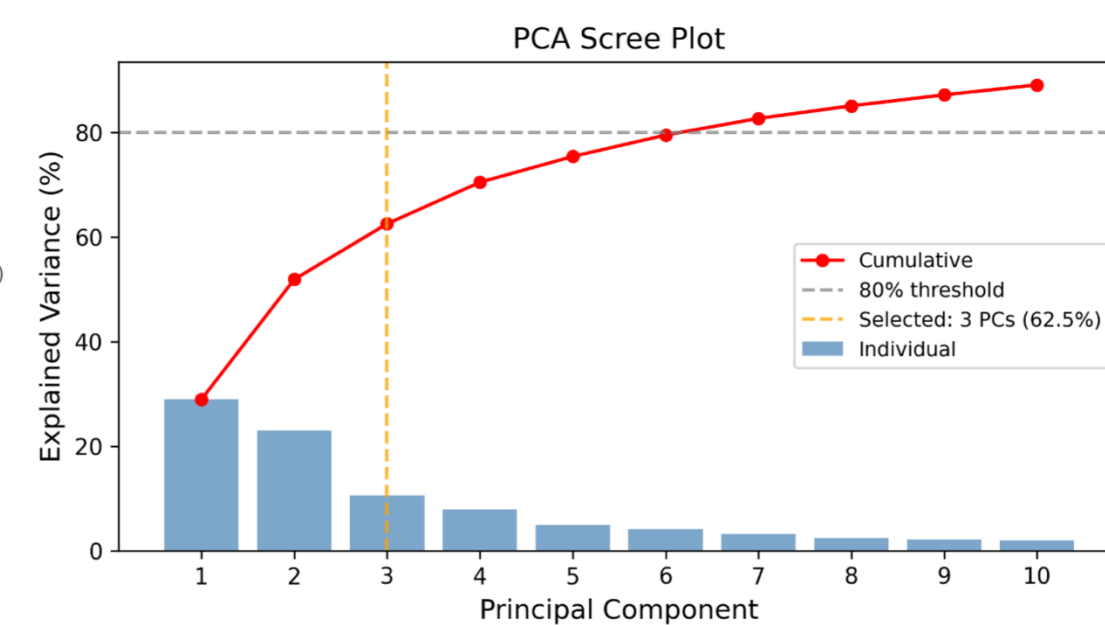


Fig. 4. PCA Scree plot.

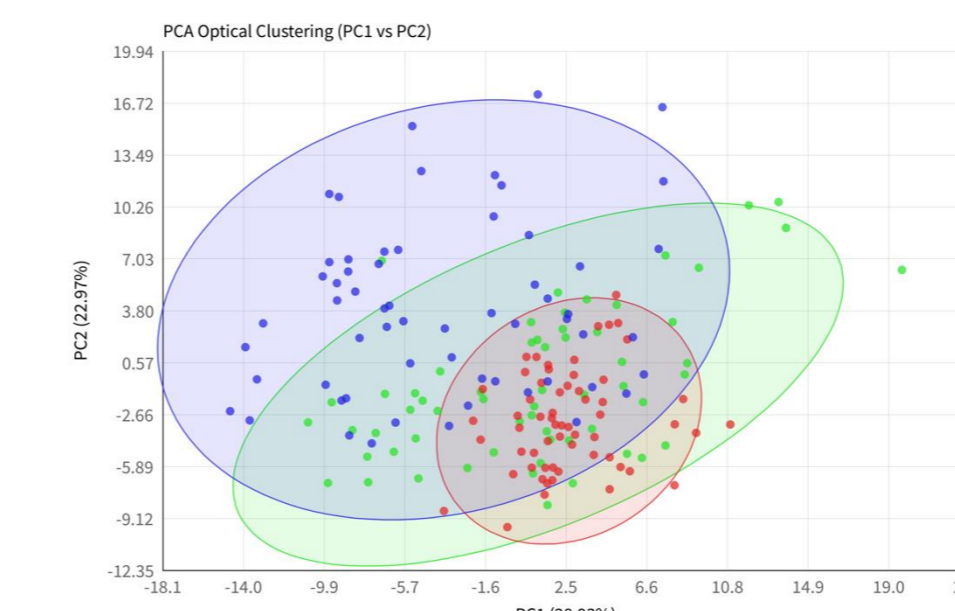


Fig. 5. PCA score plots with 95% confidence ellipses for Kozo (red), Mitsumata (blue), and Gampi (green): PC1 vs. PC2

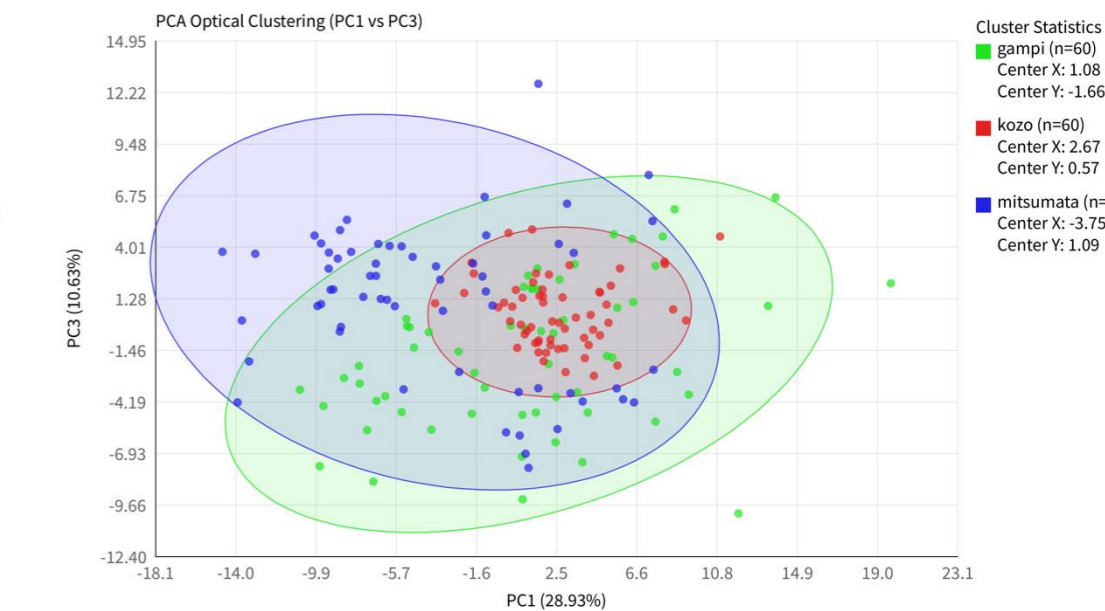


Fig. 6. PCA score plots with 95% confidence ellipses for Kozo (red), Mitsumata (blue), and Gampi (green): PC1 vs. PC3

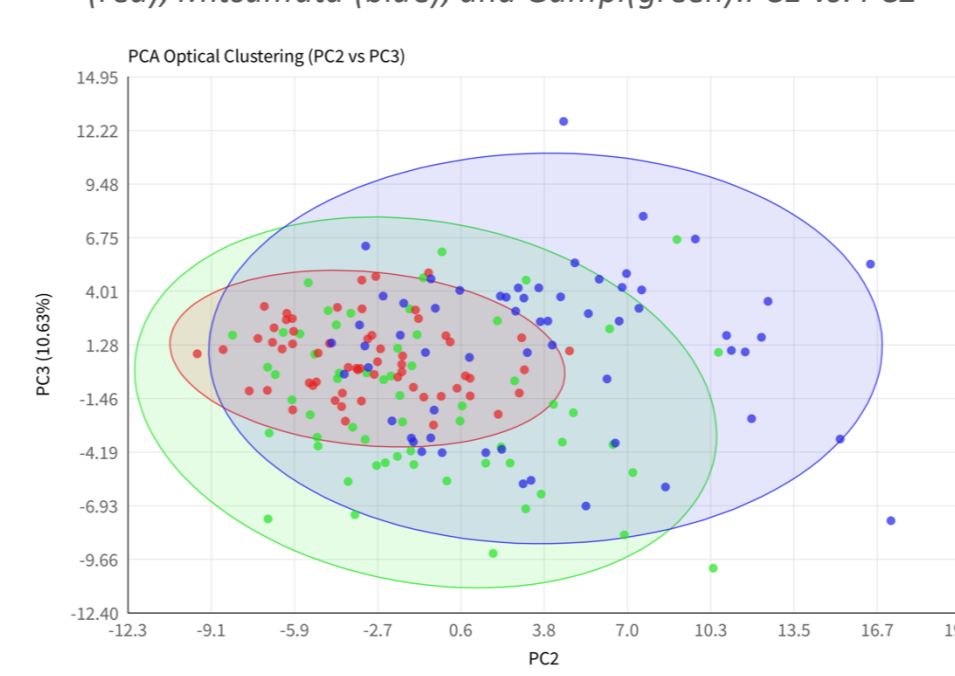


Fig. 7. PCA score plots with 95% confidence ellipses for Kozo (red), Mitsumata (blue), and Gampi (green): PC2 vs. PC3

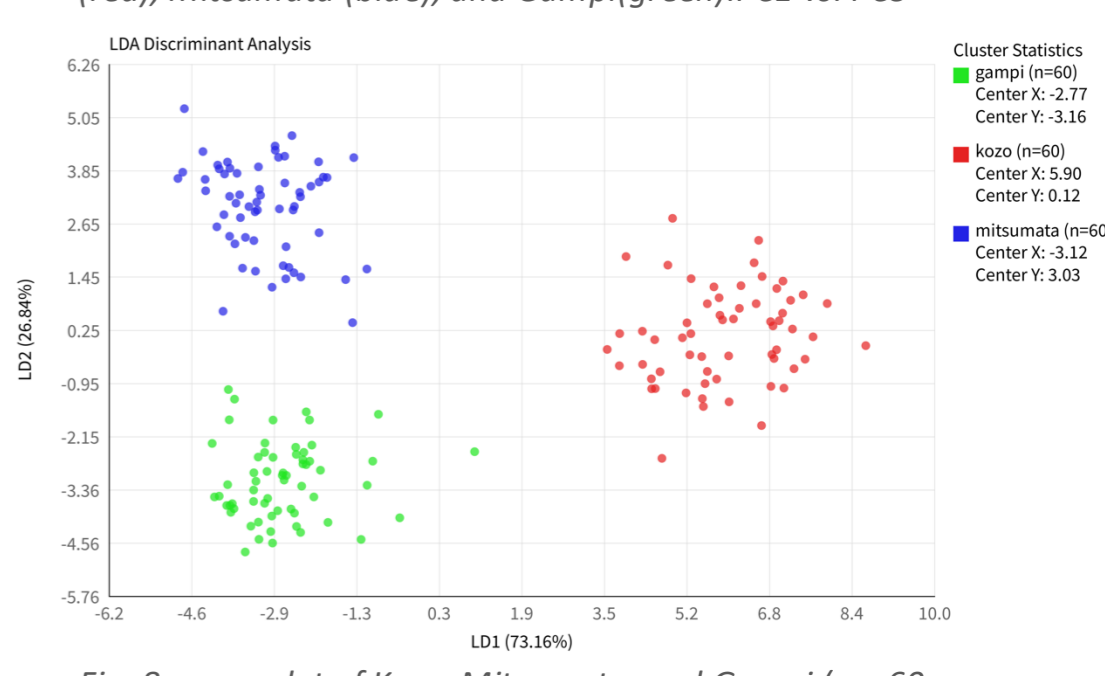


Fig. 8. score plot of Kozo, Mitsumata, and Gampi (n = 60 per class). All three fiber types form distinct clusters, with LD1 (73.16%) and LD2 (26.84%) providing effective species-level discrimination.

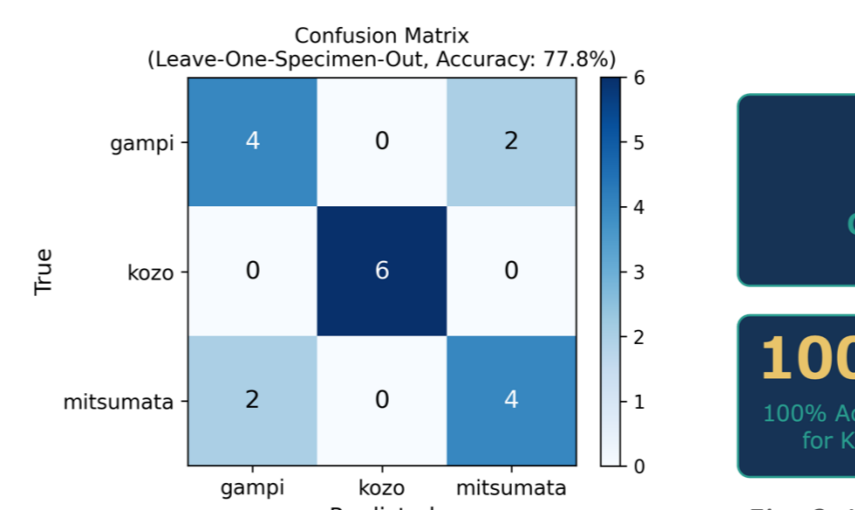


Fig. 9. LOSO-CV confusion matrix.

CONCLUSION

- Micro-HSI + chemometrics enables non-destructive, physicochemically interpretable fiber discrimination at the single-fiber scale.
- Establishes a controlled microscopic spectral reference to support future analysis of historical paper.

FUTURE WORK / REFERENCES

Future work

- Extend to naturally aged and historical specimens.
- Spectral unmixing for mixed-pulp documents; expanded reference datasets.
- Adapt acquisition for bound volumes and fragile artifacts.

References

- Wu et al., Carbohydr. Polym. 2025, 352, 123198.
- Kamiya et al., NDT 2024, 2, 487–503.
- Sadeghifar & Ragauskas, Polymers 2020, 12, 1134.
- Schwanninger et al., J. Near Infrared Spectrosc. 2011, 19, 287–308.